

AGIC: Approximate Gradient Inversion Attack on Federated Learning

Jin Xu, Chi Hong, Jiyue Huang, Lydia Y. Chen, Jérémie Decouchant

Delft University of Technology, The Netherlands

j.xu-21@student.tudelft.nl, {c.hong, j.huang-4, y.chen-10, j.decouchant}@tudelft.nl

Abstract—Federated learning is a private-by-design distributed learning paradigm where clients train local models on their own data before a central server aggregates their local updates to compute a global model. Depending on the aggregation method used, the local updates are either the gradients or the weights of local learning models, e.g., FedAvg aggregates model weights. Unfortunately, recent reconstruction attacks apply a gradient inversion optimization on the gradient update of a single mini-batch to reconstruct the private data used by clients during training. As the state-of-the-art reconstruction attacks solely focus on single update, realistic adversarial scenarios are overlooked, such as observation across multiple updates and updates trained from multiple mini-batches. A few studies consider a more challenging adversarial scenario where only model updates based on multiple mini-batches are observable, and resort to computationally expensive simulation to untangle the underlying samples for each local step. In this paper, we propose AGIC, a novel Approximate Gradient Inversion Attack that efficiently and effectively reconstructs images from both model or gradient updates, and across multiple epochs. In a nutshell, AGIC (i) approximates gradient updates of used training samples from model updates to avoid costly simulation procedures, (ii) leverages gradient/model updates collected from multiple epochs, and (iii) assigns increasing weights to layers with respect to the neural network structure for reconstruction quality. We extensively evaluate AGIC on three datasets, namely CIFAR-10, CIFAR-100 and ImageNet. Our results show that AGIC increases the peak signal-to-noise ratio (PSNR) by up to 50% compared to two representative state-of-the-art gradient inversion attacks. Furthermore, AGIC is faster than the state-of-the-art simulation-based attack, e.g., it is 5x faster when attacking FedAvg with 8 local steps in between model updates.

Index Terms—reconstruction attack, federated learning, federated averaging

I. INTRODUCTION

Federated learning (FL) [1]–[5] is a popular collaborative learning paradigm that aims at providing accurate predictive models while preserving the clients’ data privacy and reducing communication costs. In a FL system, the training data of a client never leaves its initial premises. In each global round, the server first sends the most recent model to clients, which then train the local model on their private data and send gradients or model updates back to the server. At the end of a global round, the server is able to update the global model by aggregating all the gradients or model updates it has received.

An attacker that would compromise the server would observe model parameters and their updates, but would not have

access to training samples. Therefore, FL is often assumed to safely protect the clients’ local data. However, recent works have shown that the observation of model parameters and gradient updates might allow attributes of local samples to be leaked [6], class representatives to be inferred [7], [8], and even real training samples to be reconstructed [9], [10].

Gradient inversion attacks that directly reconstruct training samples based on a model and gradient updates on it result in the most serious data leakages. Most gradient inversion attacks are optimization-based. In an optimization-based gradient inversion attack, the adversary randomly initializes dummy samples, and executes forward and backward propagation on them to obtain dummy gradients. The dummy samples are then optimized to minimize the sum of the distance between the observed real gradients and the dummy gradients, and regularization terms. To improve the reconstruction performance, some works define new distance functions and regularization terms [10], while others exploit prior knowledge, e.g., by using batch normalization data [11] or pre-trained generative models [12].

Gradient inversion attacks are designed to reconstruct samples from gradient updates. However, in practice, federated learning systems often use federated averaging (FedAvg) [4] where clients send model updates after conducting multiple local steps, each executed over a mini-batch, in order to further reduce the communication overhead. Few previous works have discussed how to attack model updates generated by FedAvg. These works either use simulation [10], which is slow and incompatible with label inference, a sub-task that significantly improves the reconstruction performance [13], or make an averaging approximation [14] to estimate the gradient of a full batch for FedAvg, which does not extend to the most general case where mini-batches are used.

In this paper, we describe AGIC, a novel Approximate Gradient Inversion Attack that specifically targets federated learning systems based on FedAvg’s model updates, and is also compatible with gradient updates. Overall, AGIC makes the following contributions.

First, to avoid the computational overhead of simulation attacks, AGIC leverages a one-batch approximation, which assimilates multiple local steps executed over multiple mini-batches as a single local step executed over a single aggregated mini-batch. The corresponding gradients of that larger mini-batch can also be approximated based on the received model update. Thanks to this one-batch approximation, AGIC is

faster than previous simulation-based attacks on FedAvg and is compatible with label inference.

Second, based on the observation that the attacker is able to observe updates across multiple epochs, AGIC better exploits the information contained in multiple updates that have been computed over common data samples. AGIC matches the collected updates with specific training samples and jointly optimizes with the updates to improve the reconstruction quality of the specific training samples.

Finally, AGIC assigns different weights to the gradients of different layers in the distance function to optimize, inspired by the results of recent works on model compression that have shown that model layers have unequal effects on model accuracy and other metrics [15], [16]. Interestingly, AGIC uses a layer weight modifier for convolutional neural networks (CNN) that use ReLU as activation function, to balance the contribution of each convolution layer, because ReLU imports zeros into gradients.

Our experiments with three datasets show that AGIC outperforms two representative state-of-the-art baselines in both reconstruction quality and efficiency. When attacking gradient updates, AGIC’s peak signal-to-noise ratio is up to 50% higher than with both baselines. When attacking FedAvg model updates configured with 8 local steps, AGIC reconstructs samples five times faster than the only applicable baseline, a state-of-the-art simulation-based attack.

The remainder of this paper is organized as follows. Section II provides some background on federated learning and gradient inversion attacks. Section III introduces our system and threat models, and an overview of AGIC. Section IV describes AGIC’s three key features. Section V evaluates AGIC’s performance. Finally, Section VII concludes this paper.

II. BACKGROUND

A. Federated learning

Federated learning (FL) [2], [5] is a collaborative learning paradigm that allows distributed data owners (called clients) to jointly learn machine learning models without centrally pooling their data. Clients train the model using their own local data and rely on a central server to aggregate their learning results. The FL system progresses over multiple global rounds. At the beginning of a global round, the server sends the latest global model to clients. Clients then train the latest model on their own data, and send their training results, i.e., gradients or model updates, back to the server.

The local training process typically follows the stochastic gradient descent (SGD) algorithm, which iterates through the data using batches. A batch might contain the full local dataset, but in the more general case a batch is a subset of the local dataset and is also called a mini-batch. During an *epoch*, clients iterate over their complete training data once. A client may use its full dataset in a single batch during one round, which is then regarded as an epoch. We focus on the more general mini-batch case, where the full dataset is split into multiple mini-batches, and the client iterates over these mini-batches in multiple global rounds during an epoch.

1. Server sends **global model W** to clients.
2. Clients train on local data, and send **gradient update ∇W** after 1 local step, or **model update W_T** after T local steps.
3. Server updates global model with updates from clients.

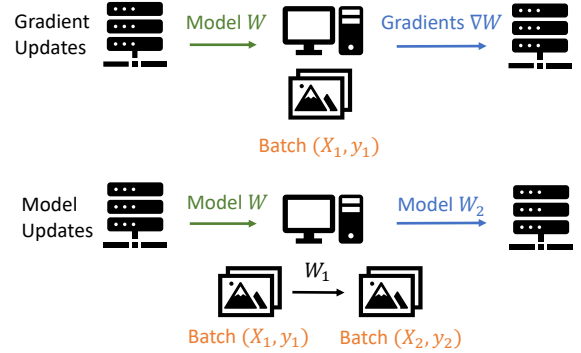


Fig. 1: A global federated learning round with gradient update and with model update.

Figure 1 depicts two typical local training procedures of FL learning systems that respectively send gradient updates after one local step (top), or send model updates after multiple local steps (bottom), which is the case with federated averaging (FedAvg) [4]. With the first method, the clients execute a single local training step on a batch of local samples and their labels (X, y) with the latest received global model W , and send back the corresponding gradient update ∇W . With FedAvg, the clients run T local steps on T batches, which means that they will update their local model parameters T times, and then send the trained model weights W_T back to the server. In practical scenarios, FedAvg is more commonly used because it reduces the amount of data transmitted over the network, in particular because a client can process several batches during a global round, i.e., before sending its results to the server. In the rest of this paper, we will note $\Delta W = W_T - W$, the difference between the updated model sent by the client at the end of a round and the global model it received at its beginning.

B. Gradient inversion attacks

Even though the clients and the server only exchange intermediate learning results such as models or gradient updates, it has been shown that sensitive information from local training datasets can be inferred in FL systems [6], [8]. Furthermore, it has been shown that an attacker that obtains gradient updates can launch a gradient inversion attack to recover the training samples that were used by clients to generate the gradients [9]. Gradient inversion attacks generally assume the attacker is an honest-but-curious server [10].

Most existing gradient inversion attacks solve an optimization problem, as illustrated in Figure 2a. After retrieving gradient updates ∇W , the attacker generates dummy samples (\hat{X}, \hat{y}) and minimizes the distance between the received gradients ∇W and its dummy gradients $\nabla W'$, which are retrieved by feeding dummy samples through the obtained model in

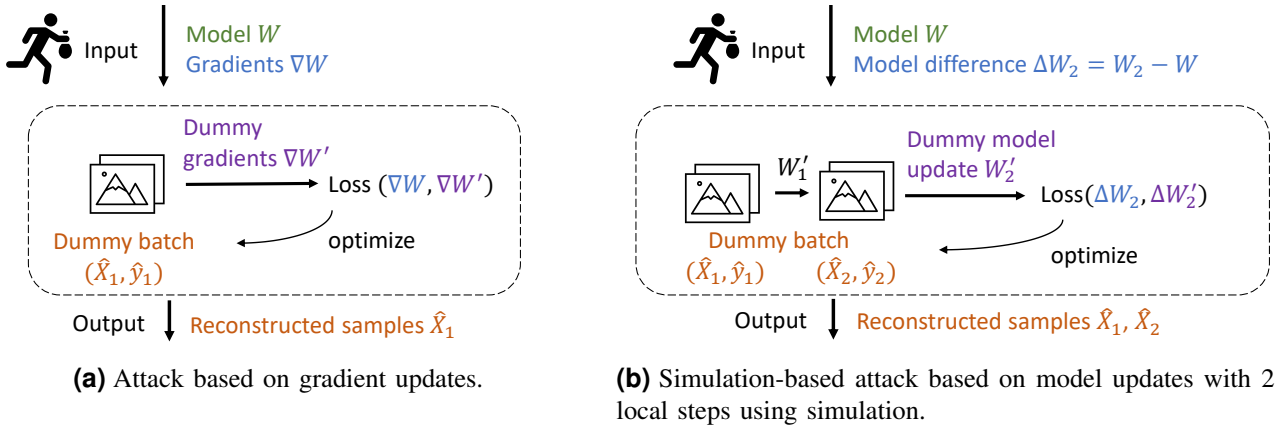


Fig. 2: Gradient inversion attacks based on gradient updates and model updates.

one forward-backward pass. During the optimization process, the values of the dummy samples are optimized, so that at the end of the attack the dummy samples approximate the training samples.

An optimization-based gradient inversion attack typically relies on an optimization objective such as:

$$\min_{\hat{X}} \text{Dist}\left(\frac{\partial \mathcal{L}(F(W, \hat{X}), \hat{y})}{\partial W}, \nabla W\right) + \text{Reg}(\hat{X}, \hat{y}) \quad (1)$$

Formula 1 uses the following notations. W is the current values of the trainable parameters of the attacked neural network. $\nabla W = \frac{\partial \mathcal{L}(F(W, X), y)}{\partial W}$ is the gradient update received from a client. F is the forward propagation function of the model. \mathcal{L} is the loss function of the model. \hat{X} is the generated reconstruction samples and \hat{y} is the labels of the samples. Dist is a distance function such as the L2 distance [9] and the cosine distance [10], which are the two most widely used distance functions in gradient inversion attacks. Reg refers to regularization terms. For attacks on image classification tasks, additional regularization terms can be leveraged to generate more natural images. For example, total variation [10] is used to reduce image noise, and clipping terms [14] are used to prevent abnormal values that are out of range for a pixel. The sum of the distance and regularization terms for generated samples forms the objective to be minimized.

In the previous paragraph, we mention that both dummy samples \hat{X} and dummy labels \hat{y} are simultaneously optimized to recover the local training data (X, y) . In reality, to avoid jointly optimizing on the labels and reducing the complexity of the optimization problem, recent analytical approaches infer the labels before conducting the optimization by analyzing the distribution of the gradient tensor of the last fully connected layer [11], [13]. Label inference is a crucial step to improve reconstruction quality of the most recent gradient inversion attacks.

Designing accurate gradient inversion attacks on model updates with mini-batches is more difficult than on gradient updates. Indeed, assuming a batch size B for each local step, an adversary attacking gradient updates needs to reconstruct B

samples. With model updates, from T local-step model updates respectively computed over T different mini-batches of size B , the adversary needs to reconstruct TB samples for an identical update size, i.e., number of model parameters.

While most gradient inversion attacks can only be applied to gradient updates, a recent attack on model updates [10] simulates the execution of T local steps in each optimization iteration, retrieves the dummy model update W'_T after the last local step, and optimizes the dummy samples in all mini-batches $\hat{X}_1, \dots, \hat{X}_T$ based on the difference between the dummy model and the observe model $\Delta W'_T = W'_T - W$ and the real observed model difference ΔW_T . Figure 2b illustrates a simulation-based gradient inversion attack based on FedAvg model updates.

III. OVERVIEW OF AGIC

This section defines our system and threat models, and provides an overview of AGIC, our gradient inversion attack.

A. System and adversarial models

We consider a FL system with one server that aggregates updates and multiple clients. We assume all clients to be correct and that the server is honest-but-curious. Therefore, our adversary observes the communications between the server and the clients and can retrieve both models and model updates. The attack can occur at any phase of the training process to target untrained, in-training or well-trained networks. The attacker may observe updates from different epochs during training. During an epoch a client iterates over its whole dataset, possibly using different mini-batches.

We focus on attacking convolutional neural networks (CNN), which are used for image classification, one of the most popular uses of FL systems. For example, it can be used by medical institutes to collaboratively train a diagnosis model [17] without sharing patient-related information.

B. Attack overview

To successfully run gradient inversion attacks on FedAvg, AGIC relies on three key features: the one-batch approximation for federated averaging, the leveraging of model updates

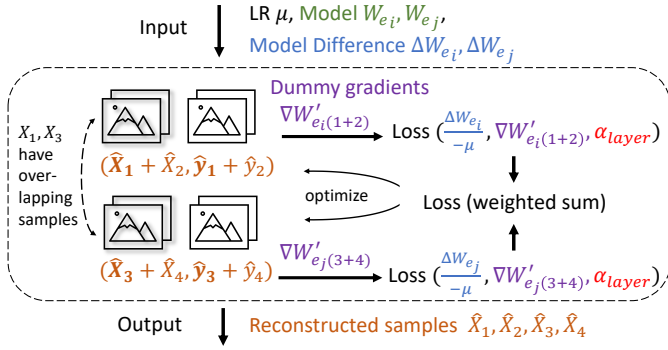


Fig. 3: Overview of AGIC.

from multiple epochs, and the assignment of layer weights in the distance function.

Figure 3 illustrates AGIC and its key features. Compared to the simulation attack on FedAvg, which was presented in Figure 2b, this Figure shows AGIC key features. First, AGIC uses a one-batch approximation so that mini-batches \hat{X}_1, \hat{X}_2 within a two-step FedAvg update compose a larger batch $\hat{X}_1 + \hat{X}_2$ (cf. §IV-A). Figure 3 also illustrates two FedAvg model updates from two different epochs e_i, e_j that have used overlapping samples in their first local step, i.e., first mini-batch, respectively X_1 and X_3 . Tensors \hat{X}_1 and \hat{X}_3 thus have overlapping components and can be jointly optimized. (cf. §IV-B). α_{layer} represent the different layer weights that AGIC uses in its distance function (cf. §IV-C).

Base loss function used during optimization. The base loss function that AGIC uses to reconstruct images from an update is the negative cosine distance between the dummy gradients $\nabla W' = \frac{\partial \mathcal{L}(F(\hat{X}, W), y)}{\partial W}$ and the received real gradients ∇W , to which is added a total variation (TV) regularization term that reduces image noises with weight ζ_{TV} [18]:

$$\min_{\hat{X}} 1 - \cos(\nabla W', \nabla W) + \zeta_{TV} \text{TV}(\hat{X}) \quad (2)$$

$$\cos(\nabla W', \nabla W) = \frac{\nabla W' \cdot \nabla W}{\|\nabla W'\|_2 \|\nabla W\|_2} \quad (3)$$

The dummy samples are optimized based on the gradient values from back propagation of the loss. AGIC modifies this base loss function to adapt to different attack scenarios.

AGIC is a novel approximate gradient inversion attack that is applicable to both model updates and gradient updates. We focus on the more challenging model update scenario, but our methods (namely, leveraging multiple epochs and choosing layer weights) also apply to gradient updates.

IV. KEY IMPLEMENTATION FEATURES OF AGIC

This section details AGIC’s three key features that enable its use with FedAvg and increase its accuracy: one-batch approximation, use of multiple updates, and layer weights.

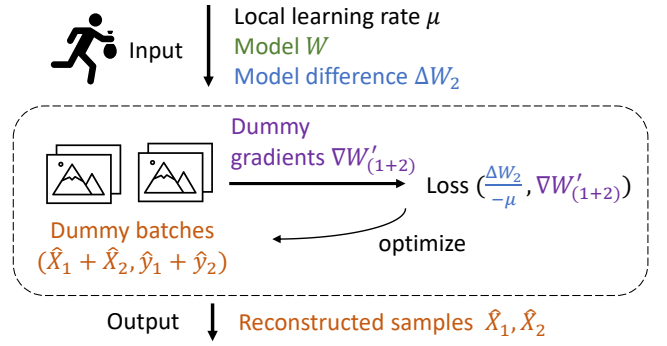


Fig. 4: Gradient inversion attack with AGIC’s one-batch approximation on FedAvg model updates. Here, clients use 2 local steps before sharing model updates with the server.

A. One-batch approximation for FedAvg

As previously explained, accurately reconstructing samples from FedAvg’s model updates is more difficult than with gradient updates because a model update is computed using more samples. When attacking FedAvg with possibly multiple local steps, AGIC is faster and more accurate than simulation-based gradient inversion attacks thanks to its one-batch approximation. This approximation allows AGIC not to use computationally expensive simulation and to be compatible with label inference, as there is no need to assign inferred labels to different local steps.

The one-batch approximation is equivalent to assuming that the model remains mostly identical after each local step. This assumption has been discussed in large mini-batch training [19]. A similar first-order approximation has been used in meta learning [20]. It should be noted that if model parameters change drastically in each local step, e.g. when the learning rate of local SGD is 1×10^{-2} , the one-batch approximation should not be used. In our experiments, with a learning rate of 1×10^{-4} , the approximation brings good performance (cf. V-B).

Figure 4 illustrates AGIC’s one-batch approximation on FedAvg’s updates. Compared to the multi-step simulation of [10], which is presented in Figure 2b, AGIC’s approximation only runs one local step with the aggregated batch, and its loss function is based on approximated gradients instead of models difference ΔW . More precisely, given all the mini-batches used in one FedAvg update X_1, \dots, X_n and their inferred labels y_1, \dots, y_n , and local learning rate μ , AGIC makes the approximation that all the mini-batches compose a larger batch $X_A = [X_1, \dots, X_n]$ to produce the received model update:

$$\Delta W \approx \sum_j^N -\mu \frac{\partial \mathcal{L}(F(W, X_j), y_j)}{\partial W} = -\mu \frac{\partial \mathcal{L}(F(W, X_A), y_A)}{\partial W} \quad (4)$$

Based on Formula 4, AGIC computes the approximated gradients $\nabla W = \frac{\Delta W}{-\mu}$ for aggregated batch X_A from the model updates given then local learning rate. Then AGIC

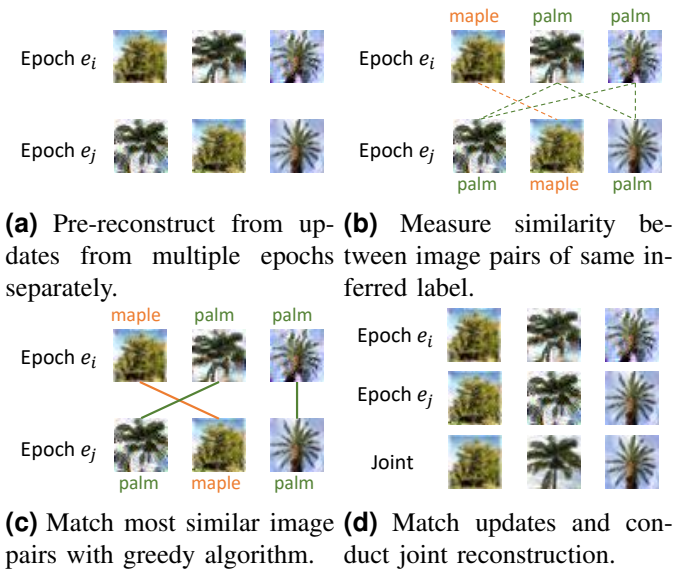


Fig. 5: Reconstruction from updates from multiple epochs. We use updates with batch size 1 for illustration purposes.

initializes dummy samples \hat{X}_A as the size of X_A , and optimizes on the distance between dummy gradients from \hat{X}_A and the computed gradients from received model updates. Because the objective function is the distance between gradients, any improvement method designed for gradient updates can be directly applied on FedAvg model updates with AGIC’s approximation.

B. Leveraging updates from multiple epochs

A training sample is used in many global rounds, each round producing an update, and thus is involved in multiple updates that are communicated to the server. The attacker can therefore observe several updates that are based on some specific samples. AGIC demonstrates that the adversary can better reconstruct the samples by making use of the updates it observes.

Prior work by Geng et al. has shown that reconstruction quality of a specific batch is improved if jointly optimizing with more pairs of model parameters W_k and their corresponding gradient update from that batch W'_k [14]. However, this method only works on full batch gradient descent and does not provide a solution to the general case where the client uses multiple mini-batches to go over its data as in an epoch. In contrast, AGIC is able to reconstruct training samples using multiple model updates or gradient updates from different mini-batches across epochs during training.

AGIC processes updates from multiple epochs in two steps: (i) *update matching*, which matches the collected updates whose corresponding samples are overlapping; and (ii) *joint reconstruction*, which reconstructs the samples from the matching updates. We discuss those two steps in the following, and Figure 5 illustrates them with a batch size equal to 1.

Step 1: Update matching. AGIC first matches updates that have overlapping samples so that they can be jointly recon-

structed afterwards. If the training process does not shuffle the samples used between epochs, or if the entire local dataset is used in a full batch, then the matching process is trivial. In the general case, a more complex algorithm is required to match gradient updates of single mini-batches or FedAvg model updates based on multiple mini-batches. AGIC’s matching mechanism first conducts a reconstruction process for each update to obtain a first reconstruction of images, and then identifies the most similar pairs of reconstructed images.

As the adversary observes updates from two complete epochs, the pre-reconstructed samples from the first epoch’s updates can be mapped one-to-one with the samples from the updates of the second epoch. Equivalently said, for any sample X_c , two updates from the two epochs have been trained on it.

To match pairs of reconstructed images, we evaluate the similarity of pairs of images by processing the images with an average pooling layer that takes average value of each small part of an image in order to mitigate noises, and computing their mean squared error. We refer the reader to §V-D, which demonstrates the performance improvement that using a pooling layer brings.

We use a simple greedy algorithm to find a one-to-one mapping between reconstructed images from two epochs. First, we measure the similarity of each image pair and sort them. From the highest similarity to the lowest one, we check each pair of still unmatched images and associate them to each other. Using this method, all pre-reconstructed images from one epoch can be matched to those from another epoch. For any matched image pairs, which are then considered to reconstruct the same sample, AGIC executes a joint reconstruction using the all updates they participated in (Step 2).

It is easy to extend this method to leverage more than two epochs, by successively computing matching update pairs from consecutive epoch pairs. A specific sample is then associated to the image pairs reconstructed from updates from consecutive epochs, and to one reconstructed image per epoch. A sample is therefore associated to exactly one update per epoch.

Since label inference can be applied before optimizing for each update, AGIC uses a label-based filter. Based on their inferred label, AGIC computes the similarity between image pairs that have the same inferred label to reduce the search space and limit the possibility of incorrect matching, thereby increasing accuracy. For a multi-sample batch, generated either from gradient update directly or from the one-batch approximation of model update, label inference returns a list of labels for all samples. Therefore, whether two samples can be matched depends on whether their inferred label lists share at least a common label.

Step 2: Joint reconstruction with multiple updates. AGIC jointly optimizes updates that have been identified as having been trained over a common sample, in order to improve reconstruction quality. We use gradients during the optimization process, obtained either from the one-batch approximation of model update or directly from received gradient update. Our distance function uses the summation of

TABLE I: PSNR results for reconstructing size-4 batches from untrained ResNet20-4, with different layer assignment functions. The decreasing functions pass through (1, 1) and $(N_{conv}, 0.5)$, and the increasing functions pass through (1, 1) and $(N_{conv}, 2)$, where the number of convolutional layers $N_{conv} = 21$ in ResNet20-4. The two points and function expressions determine the used functions.

Monotonicity	Convexity	Function	CIFAR-10	CIFAR-100
None	None	$y = 1$	14.836	15.190
Decrease	Convex	$-a \log x + b$	14.182	14.332
Decrease	Concave	$-ae^x + b$	14.727	15.175
Decrease	None	$-ax + b$	14.354	14.471
Increase	Convex	$ae^x + b$	15.255	16.001
Increase	Concave	$a \log x + b$	15.505	16.311
Increase	None	$ax + b$	15.601	16.702

distance of all pairs of input gradients and dummy gradients, with weights γ_i assigned. A decreasing weight is assigned to the gradients generated later during the training process, because the reconstruction quality of gradient inversion attacks is higher in the earliest training phases. These gradient weights are set as experimental hyperparameters (§V details the values we use).

Let us assume that after the update matching step, AGIC has identified that gradients ∇W_i with corresponding model parameters W_i from different epochs have been trained over a given sample X_c . We note $\nabla W'_i$ the dummy gradients from the dummy batches. AGIC’s distance function with multiple gradient updates is the following.

$$\min_{\hat{X}_k} \sum_k \left(1 - \frac{\nabla W'_k \cdot \nabla W_k}{\|\nabla W'_k\|_2 \|\nabla W_k\|_2} \right) \cdot \gamma_k \quad (5)$$

The reconstruction results of AGIC’s joint reconstruction are of higher quality than those that would be obtained by separately optimizing based on single updates. To illustrate why, let us consider two gradient updates from two epochs that are respectively trained from batches X_1, X_2 with overlapping sample X_c . In this situation, dummy sample \hat{X}_c is a common component of dummy batches \hat{X}_1, \hat{X}_2 and always has a single value in each dummy batch during optimization. Therefore, both updates provide information that AGIC uses to optimize the sample.

If updates are observed in two or more complete epochs then all training samples can be better recovered thanks to the update matching and joint reconstruction steps. Note that an update is used B times to jointly reconstruct different samples if the batch size is equal to B .

C. Assigning layer weights

It has been observed that different layers of a neural network have variable impact on model accuracy [16], energy consumption [15], and can be selectively pruned for model compression [21]. Similarly, we observe that gradients from different layers have different effect on the performance of a gradient inversion attack.

Based on these previous works, AGIC assigns different weights α_i to layers in the distance function used in the gradient inversion attack. For a CNN that has N_{conv} convolutional layers before the fully connected layers, suppose that the input gradients can be decomposed by layers from first to last as $\nabla W = (\nabla L_1, \dots, \nabla L_{N_{conv}}, \nabla L_{fc})$ and so do the reconstructed gradients $\nabla W'$. AGIC’s negative cosine similarity objective with layer weights α_i is indicated in Formula 6.

$$\min_{\hat{X}} 1 - \frac{\sum_i \alpha_i (\nabla L'_i \cdot \nabla L_i)}{\sqrt{\sum_i \alpha_i \|\nabla L'_i\|_2^2} \sqrt{\sum_i \alpha_i \|\nabla L_i\|_2^2}} \quad (6)$$

Linear assignment. It is impractical to separately select a weight for each layer using tedious methods like grid search. Therefore, we use a function to assign the weights to convolutional layers, and set weights of fully connected layers to the average of convolutional layer weights.

Both the shape and the range of the weight function affect performance. For the range, we first determine that the function passes through points (1, 1) and (N_{conv}, β) . Parameter β controls the range of the function and $\beta = 1$ implies homogeneous weights. We also look into various function shapes, such as linear functions $y=ax+b$, exponential-like functions $y=ae^x+b$ and logarithmic-like functions $y=a \log x+b$ to cover various function shapes (e.g., concave or convex). The two points (1, 1) and (N_{conv}, β) determine values of coefficients a, b in the various functions.

Table I presents some results obtained with different function shapes. We experimentally observe that an increasing linear weight function maximizes the reconstruction performance, and therefore determines a layer’s weight using Formula 7.

$$l_i = 1 + \frac{\beta - 1}{N_{conv} - 1} (i - 1) \quad (7)$$

In practice, the properties of the attacked network change during the training process. For example, the magnitude of gradient values becomes smaller and the reconstruction quality deteriorates. In consequence, the best value for parameter β changes according to the attacked training phase (as illustrated in Figure 9).

ReLU modifier. We can directly set $\alpha_i=l_i$ in the general case, but we additionally propose a layer weight modifier for CNNs that apply ReLU after convolution layers, as $\text{ReLU}(x) = \max(0, x)$ is the most commonly used activation function in current CNN designs such as ResNet [22]. ReLU is more popular than sigmoid functions, because it simplifies gradient computation in backward propagation and avoids gradient vanishing and gradient inversion.

When the input of ReLU is negative, its output is set to zero, and as a result, after back propagation, the gradients of input are also equal to zero. Therefore, a proportion of zeros exists in each convolution layer’s gradients. These zeros limit the performance of gradient inversion attacks, because it is then easier for the optimization process to get its dummy

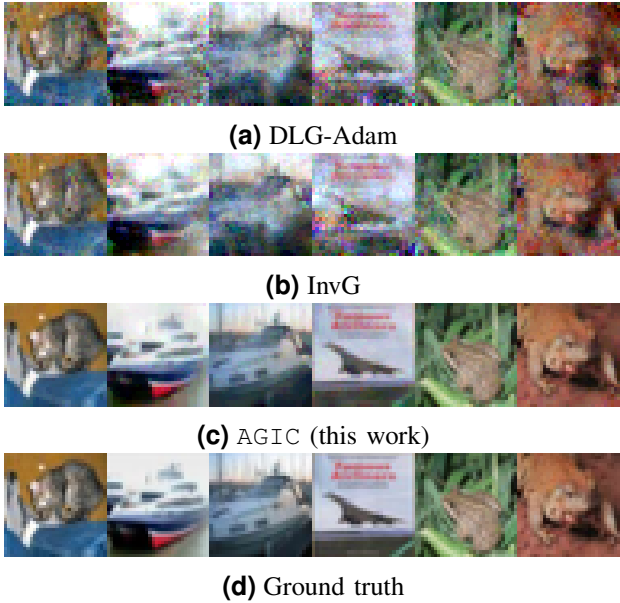


Fig. 6: Reconstructed CIFAR-10 images from untrained ResNet20-4 with batch size 1.

gradients to achieve these zeros, which appear as soon as the corresponding output of a convolutional layer is negative. Thus, layers that have more zero gradients contribute less in the reconstruction.

To remove the effect of zeros imported by ReLU and balance the contribution of each convolutional layer, AGIC relies on a layer weight modifier based on the proportion of zeros of each layer. Assuming that the proportion of zeros in a convolutional layer’s gradients is p_i , its modifier zero-based coefficient is computed as $z_i = \frac{1}{1-p_i}$.

In conclusion, the layer weight for the i -th convolutional layer is equal to a linearly assigned weight l_i , which is multiplied by a zero-based weight z_i if ReLU is used, and the layer weight of a fully connected layer is the average of the linearly assigned weights of convolutional layers:

$$\begin{aligned} \alpha_i &= l_i \cdot \frac{1}{1-p_i} && i\text{-th convolutional layer} \\ \alpha_{fc} &= \frac{\sum_{i=1}^{N_{conv}} l_i}{N_{conv}} && \text{fully connected layers} \end{aligned} \quad (8)$$

V. PERFORMANCE EVALUATION

A. Setup

Hardware. We use a machine equipped with an AMD EPYC 7542 32-core CPU, 256GB of RAM and an NVIDIA GeForce RTX 2080 Ti GPU for our experiments.

Datasets. We conduct experiments on three image datasets: CIFAR-10 (size 32×32 , 10 classes) [23], CIFAR-100 (size 32×32 , 100 classes) [23], and ImageNet (size 224×224 , 1000 classes) [24]. All three datasets contain 3-channel colored images. The datasets are normalized to mean 0 and standard deviation 1. For the experiments, we randomly select 100 mini-batches from the validation set of each dataset. We attack

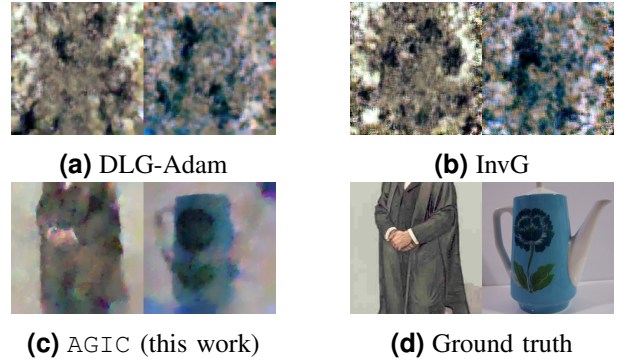


Fig. 7: Reconstructed ImageNet images from untrained ResNet50 with batch size 1.

ResNet trained on the datasets [22]: ResNet20-4 on CIFAR-10 and CIFAR-100, and ResNet50 on ImageNet.

Baselines. We compare our attack with two baselines. The first is an improved version of DLG [9], namely DLG-Adam, which uses the Adam optimizer instead of L-BFGS in the original version, because L-BFGS often fails to converge while attacking large networks like ResNet [10]. The other baseline is Inverting Gradients [10], which we call InvG. The two baselines cover the two main distance functions applied in gradient inversion attacks.

We do not compare our attack to those based on pretrained models, e.g., an image generative model [12], because we do not assume the attacker to have access to additional knowledge. We also do not consider a batch normalization (BN) regularization term [11], because it requires that each synchronous BN layer has cross-node communication during forward propagation, which is very time-consuming and impractical in FL. Our methods are however orthogonal to these methods that leverage extra information and could be combined with them.

Hyperparameters. The Adam optimizer with learning rate 0.1 is used based on the gradient values on dummy samples during optimization. ζ_{TV} is equal to 10^{-4} for untrained ResNet20-4, 10^{-2} for trained ResNet20-4, 10^{-3} for untrained ResNet50, and 10^{-1} for trained ResNet50. For FedAvg, the learning rate of local SGD is $\mu = 1 \times 10^{-4}$. The kernel size of the averaging pooling layer used in update matching is 2×2 and the stride of it is 2. Regarding epoch weights γ_i in multi-epoch reconstruction, $\gamma = 1$ for a batch from the first epoch, and $\gamma = 0.1$ for the other batches. For layer weights, $\beta = 50$ for untrained networks, and $\beta=2$ for trained networks. The optimization has 10,000 iterations.

Because label inference is an independent subtask that has already been well explored and for which very accurate methods already exist, we assume that labels are correctly inferred in experiments of gradient updates, if not specified in other ways. For our experiments with FedAvg, we apply the label inference method from [11]. Labels in a mini-batch are assumed not to be duplicated, following the experiment setup of previous works [10], [11].

TABLE II: Reconstruction quality of gradient inversion attacks on untrained ResNet20-4 on CIFAR-10 and CIFAR-100, and trained ResNet50 on ImageNet, on FedAvg model updates. Here, FedAvg runs on 4 size-1 mini-batches and 4 local steps.

Method	simulation	CIFAR-10, untrained			CIFAR-100, untrained			ImageNet, trained		
		PSNR \uparrow	SSIM \uparrow	LPIPS \downarrow	PSNR \uparrow	SSIM \uparrow	LPIPS \downarrow	PSNR \uparrow	SSIM \uparrow	LPIPS \downarrow
DLG-Adam	✓	13.611	0.391	0.123	15.114	0.463	0.096	8.044	0.028	1.314
InvG	✓	14.108	0.414	0.117	15.465	0.480	0.092	10.593	0.167	0.779
AGIC (this work, one-batch)	×	14.250	0.414	0.115	15.437	0.475	0.093	10.522	0.161	0.791
AGIC (this work, one-batch + layers)	×	16.182	0.529	0.112	19.133	0.672	0.050	10.699	0.177	0.780

TABLE III: Reconstruction quality of gradient inversion attacks on FedAvg, with local step 4 and batch size 2, on ResNet20-4 on CIFAR-100. The matching batches from two epochs are assumed to have the same samples. A '1' in the Epochs column means that the updates are collected after one epoch, while '1, 2' means that the matching updates are collected after one epoch and two epochs.

Method	Simulation	Epochs	PSNR \uparrow	SSIM \uparrow	LPIPS \downarrow
DLG-Adam	✓	1	12.196	0.292	0.087
InvG	✓	1	14.398	0.419	0.065
AGIC (this work)	×	1	15.651	0.486	0.055
AGIC (this work)	×	1,2	16.664	0.533	0.040

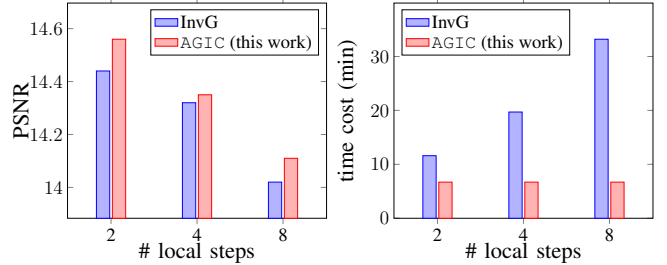
TABLE IV: Reconstruction quality of gradient inversion attacks on single gradient updates, reconstructing CIFAR-10 images from untrained ResNet20-4 and ImageNet images from untrained ResNet50.

Dataset	Batch size	Method	PSNR \uparrow	SSIM \uparrow	LPIPS \downarrow
CIFAR-10	1	DLG-Adam	19.908	0.727	0.034
		InvG	20.671	0.753	0.031
		AGIC (this work)	31.341	0.963	0.004
CIFAR-10	4	DLG-Adam	14.034	0.412	0.110
		InvG	14.421	0.433	0.103
		AGIC (this work)	17.183	0.586	0.092
ImageNet	1	DLG-Adam	11.311	0.094	0.751
		InvG	12.832	0.214	0.691
		AGIC (this work)	15.573	0.366	0.670
ImageNet	4	DLG-Adam	9.879	0.070	0.801
		InvG	11.640	0.216	0.720
		AGIC (this work)	12.836	0.302	0.721

Metrics. We use three metrics to measure the similarity between the reconstructed images and the real training samples: (i) peak signal-to-noise ratio (PSNR), (ii) structural similarity index measure (SSIM) [25], and (iii) LPIPS, a perceptual image similarity score [26]. Higher PSNR, higher SSIM, and lower LPIPS all indicate better reconstruction quality.

B. Overall performance of AGIC

We first report the overall performance of AGIC on FedAvg model updates and Gradient updates. Table II shows the attack results on single FedAvg model updates. The one-batch approximation and layer weights are used with this FL setting. AGIC with the one-batch approximation outperforms the other



(a) Reconstruction quality. **(b)** Computation time for attacks with 10k iterations.

Fig. 8: Reconstruction qualities and computation times for the simulation-based attack InvG and for AGIC on CIFAR-10 images from untrained ResNet20-4. Each model update is generated with 8 images, e.g., for the 8-step scenario each update is generated from 8 size-1 mini-batches.

two baselines that are based on simulation of FedAvg. Table III further shows the attack results on FedAvg with updates from multiple epochs. One can also observe that AGIC further increases its reconstruction quality when reconstructing from matching updates from multiple epochs.

AGIC can also attack gradient updates, the most common setup in gradient inversion attacks, as shown in Table IV. These results are interesting because only layer weights are used in this experiment, and AGIC significantly outperforms baseline methods, with different datasets and batch sizes. AGIC improves the PSNR over CIFAR-10's by up to almost 50%. The reconstructed CIFAR-10 samples in Figure 6 are visually almost identical to the ground truth. Figure 7 shows two examples of reconstructed ImageNet samples, where AGIC also clearly outperforms the baselines.

C. Computation time reduction with the one-batch approximation

We further compare the one-batch approximation of AGIC with the simulation approach of InvG, for attacking FL systems using FedAvg. We look into the case where a FedAvg update is generated from 8 images, but they are divided into mini-batches with different sizes in different experiments, which implies that the number of local steps also changes. Figure 8 show that AGIC outperforms InvG in both quality and speed with all settings. It can also be noticed that both

TABLE V: Matching success rate of 1000 CIFAR-100 images from epochs 1 and 2, with different update matching methods and batch sizes.

Labels	Pooling	Batch size 1	Batch size 4
×	×	0.819	0.509
×	✓	0.873	0.547
✓	×	0.988	0.672
✓	✓	0.981	0.705

TABLE VI: Reconstruction quality with 200 CIFAR-100 images using gradients from epochs 1 and 2, using label inference and update matching, and equal layer weights. The model is ResNet20-4 and the batch size equals 1.

Epochs	PSNR↑	SSIM↑	LPIPS↓
1	20.379	0.665	0.026
2	19.085	0.626	0.022
1,2	21.464	0.697	0.016

methods have worse performance when the number of local steps increases, if the total number of samples are fixed.

When the number of local steps increases, the time cost of attacks based on simulation also increases, while the one-batch approximation implies that AGIC has a constant time cost. When FedAvg has 8 local steps, AGIC is 5 times faster than InvG: AGIC requires 6.7 minutes on an NVIDIA GeForce RTX 2080 Ti GPU instead of 33.2 minutes with InvG.

D. Reconstruction quality improvement with update matching and joint reconstruction

We now focus on reconstructing samples from multiple epochs. We first conduct experiments on our pre-reconstruction matching method with 2,000 iterations. We consider matching with and without using an average pooling layer, and with and without restriction on inferred labels. Table V presents the matching rate with pre-reconstructed CIFAR-100 images. It shows that with pre-reconstruction, the matching rate is very high (0.988) when the batch size is 1. When the batch size is 4, the matching rate decreases (0.672), because reconstruction quality decreases when the batch size increases, but it is still high. Using inferred labels provides strong prior knowledge for gradient matching, even when the batch size is larger than 1, which implies that labels may be incorrectly inferred. A pooling layer successfully mitigates noise, except in the case where the batch size equals 1 and labels are used, which already has an almost perfect accuracy.

We further evaluate on a full setup that includes label inference the matching of gradient updates and joint reconstruction. Pre-reconstruction runs 2,000 iterations. Gradient updates are matched based on pre-reconstructed single images. Table VI shows that the reconstruction results based on two updates from two epochs are better than with single updates from either epoch (e.g., PSNR of 21.464 instead of 20.379 or 19.085).

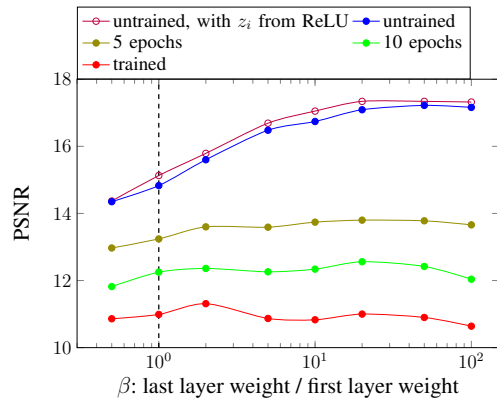


Fig. 9: Effect of different layer weights on PSNR with different experimental settings, including untrained and trained networks.



Fig. 10: Reconstructions of a CIFAR-10 image of a horse from untrained ResNet20-4 with a weight ratio β that ranges from 1 (left) to 20 (right).

E. Reconstruction quality improvement with layer weights

We investigate the effect of layer weights on reconstruction quality by varying the ratio β between the weights of the last convolutional layer and the first one, using ResNet20-4 on CIFAR-10. Figure 9 presents our results. The effect of layer weights is very significant on the untrained network. As training continues, the effect of weights weakens, and the best β value is also lower. However, assigning larger weights to later convolutional layers ($\beta > 1$) still improves performance, compared with the equally assigned weights at $\beta = 1$, even in trained networks. Figure 10 shows the reconstructed images of one CIFAR-10 sample on untrained ResNet20-4, with increasing β values. One can notice that the reconstruction quality improves when β increases.

Figure 9 also compares attacking untrained ResNet20-4 with and without ReLU weight modifier z_i . The zero-proportion-based weight modifier consistently improves the attack performance, bringing up to 2.0% improvement on PSNR.

VI. RELATED WORK

A. Gradient inversion attack on gradient updates

Gradient inversion attacks on federated learning systems reconstruct training samples from gradient updates. Deep Leakage from Gradients (DLG) [9] is the first gradient inversion attack. DLG jointly optimizes on the samples and on the labels, which complicates the optimization objective and impairs the reconstruction quality if the labels are inaccurately optimized. Improved DLG (iDLG) [13] proposes to conduct label inference before DLG’s optimization and shows that labels can be

TABLE VII: Comparison of AGIC and other gradient inversion attacks on (horizontal) federated learning systems.

Method	Main loss term	Other loss terms	Optimizer	Label inference capability	Extra knowledge	Trained network	Multiple epochs' updates	FedAvg
DLG [9]	L2	None	L-BFGS	No use	No	×	×	×
iDLG [13]	L2	None	L-BFGS	One	No	×	×	×
Inverting Gradients (InvG in this paper) [10]	Cosine	Total variation	Adam	One	No	✓	×	✓
CPL [27]	L2	Label-based	L-BFGS	One	No	×	×	×
R-GAP [28]	Recursively	N/A	N/A	One	No	×	×	×
Grad-Inversion [11]	L2	Total variation, L2 of input, BN, group consistency	Adam	Multiple	BN statistics, pretrained image alignment model	✓	×	×
Geng et al. [14]	L2	Clipping, scaling	L-BFGS	Multiple	No	×	×	Only full batch
GIAS [12]	Cosine	Total variation	Adam	One	Pretrained generative model	×	×	×
AGIC (this work)	Cosine	Total variation	Adam	Multiple	No	✓	✓	✓

inferred with perfect accuracy using some analytical method when the batch size is equal to 1. Following iDLG, several label inference methods explained how to infer labels in larger batches with higher accuracy [11], [14], [29]. Label inference is now an essential part of current gradient inversion attacks since it significantly improves the reconstruction quality.

Most existing gradient inversion attacks are optimization-based: they formulate an optimization problem and minimize the distance between the real observed gradient update and a dummy gradient update in order to optimize the reconstructed samples. Therefore, one way to improve the performance of a gradient inversion attack is to design a better objective function. Geiping et al. uses the cosine distance instead of L2 distance in DLG [10]. CPL adds a label-based regularization term to improve the optimization stability [27]. Another way to improve the reconstruction performance is to leverage prior knowledge in specific scenarios. GradInversion adds a batch normalization regularizer, because the attacker is assumed to know batch normalization statistics, and it designs a group consistency regularization term leveraging multiple reconstruction processes with different initialization seeds to find an enhanced reconstruction result [11]. GIAS assumes a known data distribution and improves the reconstruction quality using a pre-trained generative model [12].

R-GAP is a gradient inversion attack that is not based on optimization. Instead, R-GAP recursively reconstructs each layer's input from the last layer to first by solving linear equations, which is limited to a batch size equal to 1 [28]. The works we have discussed so far consider horizontal FL systems [3], [30] where client datasets share a given feature space. Differently, CAFE is a gradient inversion attack [31] for vertical FL systems where client datasets have different feature spaces [32], [33].

Table VII compares our attack, AGIC, with existing gradient inversion attacks, and shows that it is applicable in more

general federated learning scenarios.

B. Gradient inversion attack on FedAvg model updates

Although using FedAvg model updates is more practical than using gradient updates, only a handful of gradient inversion attacks on FedAvg's model updates have been described.

To be compatible with the multiple local steps of FedAvg, Geiping et al. simulate the local training process of multiple local steps to obtain a dummy model update, and then minimize the distance between the dummy model update and the real model update [10]. However, this method is incompatible with label inference because it is unable to associate correct labels to each mini-batch, as label inference returns a set of labels for all mini-batches. In addition, the computation time of simulation-based attacks also increases with the number of local steps FedAvg uses, because the computation graph for a model update then also gets larger [10]. Geng et al. present an attack that targets FedAvg systems that use full batch gradient descent [14]. Their attack divides the received model update by the number of local steps to approximate the model update of each local step, which is then used to approximate the full batch's gradient update. However, this attack cannot cover the common case where FedAvg uses multiple mini-batches.

AGIC addresses the limitations of previous attacks on FedAvg. First, its one-batch approximation is compatible with label inference. Second, AGIC can be used in common FedAvg scenarios that use several mini-batches per round, and it is faster than simulation-based attacks.

VII. CONCLUSION

In this paper, we presented AGIC, an accurate and fast gradient inversion attack that can leverage both model updates and gradient updates across multiple epochs. AGIC uses a one-batch approximation to convert model updates into approximate gradient updates of a larger mini-batch.

AGIC also leverages updates from multiple epochs with update matching to jointly reconstruct specific training samples accurately. Finally, AGIC assigns different weights to layers in the objective function, which significantly improves the reconstruction quality. Compared to previous works, AGIC can be used with more general federating learning system settings. Our experiments demonstrate that AGIC reconstructs samples with up to 50% PSNR improvement compared to state-of-the-art baselines, and is up to 5x faster than simulation-based attacks, which is the only baseline that can attack FedAvg.

REFERENCES

- [1] K. Bonawitz, H. Eichner, W. Grieskamp, D. Huba, A. Ingerman, V. Ivanov, C. Kiddon, J. Konečný, S. Mazzocchi, B. McMahan, *et al.*, “Towards federated learning at scale: System design,” *Proceedings of Machine Learning and Systems*, vol. 1, pp. 374–388, 2019.
- [2] K. Bonawitz, V. Ivanov, B. Kreuter, A. Marcedone, H. B. McMahan, S. Patel, D. Ramage, A. Segal, and K. Seth, “Practical secure aggregation for privacy-preserving machine learning,” in *ACM SIGSAC CCS*, 2017.
- [3] J. Konečný, H. B. McMahan, F. X. Yu, P. Richtárik, A. T. Suresh, and D. Bacon, “Federated learning: Strategies for improving communication efficiency,” *arXiv preprint arXiv:1610.05492*, 2016.
- [4] B. McMahan, E. Moore, D. Ramage, S. Hampson, and B. A. y Arcas, “Communication-efficient learning of deep networks from decentralized data,” in *Artificial intelligence and statistics*, PMLR, 2017, pp. 1273–1282.
- [5] H. B. McMahan, E. Moore, D. Ramage, and B. A. y Arcas, “Federated learning of deep networks using model averaging,” *arXiv preprint arXiv:1602.05629*, 2016.
- [6] L. Melis, C. Song, E. De Cristofaro, and V. Shmatikov, “Exploiting unintended feature leakage in collaborative learning,” in *2019 IEEE Symposium on Security and Privacy (SP)*, IEEE, 2019, pp. 691–706.
- [7] B. Hitaj, G. Ateniese, and F. Perez-Cruz, “Deep models under the gan: Information leakage from collaborative deep learning,” in *Proceedings of the 2017 ACM SIGSAC Conference on Computer and Communications Security*, 2017, pp. 603–618.
- [8] Z. Wang, M. Song, Z. Zhang, Y. Song, Q. Wang, and H. Qi, “Beyond inferring class representatives: User-level privacy leakage from federated learning,” in *IEEE INFOCOM 2019-IEEE Conference on Computer Communications*, IEEE, 2019, pp. 2512–2520.
- [9] L. Zhu and S. Han, “Deep leakage from gradients,” in *Federated learning*, Springer, 2020, pp. 17–31.
- [10] J. Geiping, H. Bauermeister, H. Dröge, and M. Moeller, “Inverting gradients-how easy is it to break privacy in federated learning?” *Advances in Neural Information Processing Systems*, vol. 33, pp. 16937–16947, 2020.
- [11] H. Yin, A. Mallya, A. Vahdat, J. M. Alvarez, J. Kautz, and P. Molchanov, “See through gradients: Image batch recovery via gradinversion,” in *Proceedings of the IEEE/CVF Conference on Computer Vision and Pattern Recognition*, 2021, pp. 16337–16346.
- [12] J. Jeon, J. Kim, K. Lee, S. Oh, and J. Ok, “Gradient inversion with generative image prior,” in *Thirty-Fifth Conference on Neural Information Processing Systems*, 2021.
- [13] B. Zhao, K. R. Mopuri, and H. Bilen, “Idlg: Improved deep leakage from gradients,” *arXiv preprint arXiv:2001.02610*, 2020.
- [14] J. Geng, Y. Mou, F. Li, Q. Li, O. Beyan, S. Decker, and C. Rong, “Towards general deep leakage in federated learning,” *arXiv preprint arXiv:2110.09074*, 2021.
- [15] T.-J. Yang, Y.-H. Chen, and V. Sze, “Designing energy-efficient convolutional neural networks using energy-aware pruning,” in *Proceedings of the IEEE conference on computer vision and pattern recognition*, 2017, pp. 5687–5695.
- [16] S. Elkerdawy, M. Elhoushi, A. Singh, H. Zhang, and N. Ray, “To filter prune, or to layer prune, that is the question,” in *Proceedings of the Asian Conference on Computer Vision*, 2020.
- [17] N. Rieke, J. Hancox, W. Li, F. Milletari, H. R. Roth, S. Albarqouni, S. Bakas, M. N. Galtier, B. A. Landman, K. Maier-Hein, *et al.*, “The future of digital health with federated learning,” *NPJ digital medicine*, vol. 3, no. 1, pp. 1–7, 2020.
- [18] L. I. Rudin, S. Osher, and E. Fatemi, “Nonlinear total variation based noise removal algorithms,” *Physica D: nonlinear phenomena*, vol. 60, no. 1-4, pp. 259–268, 1992.
- [19] P. Goyal, P. Dollár, R. Girshick, P. Noordhuis, L. Wesolowski, A. Kyrola, A. Tulloch, Y. Jia, and K. He, “Accurate, large minibatch sgd: Training imagenet in 1 hour,” *arXiv preprint arXiv:1706.02677*, 2017.
- [20] C. Finn, P. Abbeel, and S. Levine, “Model-agnostic meta-learning for fast adaptation of deep networks,” in *International conference on machine learning*, PMLR, 2017, pp. 1126–1135.
- [21] S. Chen and Q. Zhao, “Shallowing deep networks: Layer-wise pruning based on feature representations,” *IEEE transactions on pattern analysis and machine intelligence*, vol. 41, no. 12, pp. 3048–3056, 2018.
- [22] K. He, X. Zhang, S. Ren, and J. Sun, “Deep residual learning for image recognition,” in *Proceedings of the IEEE conference on computer vision and pattern recognition*, 2016, pp. 770–778.
- [23] A. Krizhevsky and G. Hinton, “Learning multiple layers of features from tiny images,” *MSc thesis, University of Toronto*, 2009.
- [24] O. Russakovsky, J. Deng, H. Su, J. Krause, S. Satheesh, S. Ma, Z. Huang, A. Karpathy, A. Khosla, M. Bernstein, *et al.*, “Imagenet large scale visual recognition challenge,” *International journal of computer vision*, vol. 115, no. 3, pp. 211–252, 2015.
- [25] Z. Wang, A. C. Bovik, H. R. Sheikh, and E. P. Simoncelli, “Image quality assessment: From error visibility to structural similarity,” *IEEE transactions on image processing*, vol. 13, no. 4, pp. 600–612, 2004.
- [26] R. Zhang, P. Isola, A. A. Efros, E. Shechtman, and O. Wang, “The unreasonable effectiveness of deep features as a perceptual metric,” in *Proceedings of the IEEE conference on computer vision and pattern recognition*, 2018, pp. 586–595.
- [27] W. Wei, L. Liu, M. Loper, K.-H. Chow, M. E. Gursoy, S. Truex, and Y. Wu, “A framework for evaluating client privacy leakages in federated learning,” in *European Symposium on Research in Computer Security*, Springer, 2020.
- [28] J. Zhu and M. Blaschko, “R-gap: Recursive gradient attack on privacy,” *arXiv preprint arXiv:2010.07733*, 2020.
- [29] T. Dang, O. Thakkar, S. Ramaswamy, R. Mathews, P. Chin, and F. Beaufays, “Revealing and protecting labels in distributed training,” *Advances in Neural Information Processing Systems*, vol. 34, 2021.
- [30] M. Kantarcioglu and C. Clifton, “Privacy-preserving distributed mining of association rules on horizontally partitioned data,” *IEEE transactions on knowledge and data engineering*, vol. 16, no. 9, pp. 1026–1037, 2004.
- [31] X. Jin, P.-Y. Chen, C.-Y. Hsu, C.-M. Yu, and T. Chen, “Catastrophic data leakage in vertical federated learning,” *Advances in Neural Information Processing Systems*, vol. 34, 2021.
- [32] J. Vaidya and C. Clifton, “Privacy preserving association rule mining in vertically partitioned data,” in *Proceedings of the eighth ACM SIGKDD international conference on Knowledge discovery and data mining*, 2002, pp. 639–644.

- [33] S. Hardy, W. Henecka, H. Ivey-Law, R. Nock, G. Patrini, G. Smith, and B. Thorne, "Private federated learning on vertically partitioned data via entity resolution and additively homomorphic encryption," *arXiv preprint arXiv:1711.10677*, 2017.